



NJC

A conjugated porphyrin as a red-light sensitizer for near-infrared emission of ytterbium (III) ion

Journal:	<i>New Journal of Chemistry</i>
Manuscript ID	NJ-ART-10-2020-004910
Article Type:	Paper
Date Submitted by the Author:	13-Aug-2020
Complete List of Authors:	Balasoorya, Dinesh ; Eastern Illinois University, Chemistry Liu, Beibei; Eastern Illinois University He, Hongshan; Eastern Illinois University, Chemistry Sykes, Andrew; University of South Dakota, Department of Chemistry May, P.; South Dakota State University College of Education and Human Sciences, Physical Chemistry Department of Chemistry

SCHOLARONE™
Manuscripts



Journal Name

ARTICLE

A conjugated porphyrin as a red-light sensitizer for near-infrared emission of ytterbium (III) ion

Dinesh Balasooriya,^{a§} Beibei Liu,^{a§} Hongshan He,^{*a} Andrew Sykes^b and P. Stanley May^b

Received 00th January 20xx,
Accepted 00th January 20xx

DOI: 10.1039/x0xx00000x

www.rsc.org/

A conjugated porphyrin with broader absorption in the visible region was synthesized for sensitizing the near-infrared emission of ytterbium (III) ion. The 4-ethynylbenzoic acid was linked to the *meso* position of a 5,15-dimesitylporphyrin resulting in a conjugated porphyrin, which has strong absorption in the visible region with an onset of up to 670 nm. After forming a complex with ytterbium (III) acetate and 1,10-phenanthroline in sulfolane, the absorption edge shifted to ~650 nm with a peak absorption at 615 nm. It was found the fluorescence from porphyrin in the visible region was almost diminished in the complex. Upon excitation at a wavelength above 600 nm, the complex showed characteristic emission at 980 nm from ytterbium (III) ion with a lifetime of 12.0 μ s in dichloromethane. The NIR emission was also observed in DMSO/water (1:1) upon excitation at 633 nm, demonstrating its potential for biological applications.

Introduction

Near-infrared (NIR, 900 – 1600 nm) emission from lanthanide ions (Yb³⁺, Er³⁺, and Nd³⁺) has potential for the detection of biological substrates when being employed as read-outs from a luminescent probe.^{1, 2} Compared to conventional visible emission from organic probes, NIR probes offer great advantages including low background signal due to low NIR emission from biological substrates,³ which could potentially lead to increased signal-to-noise ratio for more sensitive detection.⁴ Sharp and fixed emission wavelengths also provide a convenient window for monitoring the signal at different samples. For example, ytterbium (III) emits at 980 nm with a narrow full width due to the inner *4f* - *4f* transition nature.⁵ This wavelength is almost unaffected by solvents, ligands, or coordination geometry. Lastly, the long decay lifetime (typically in tens of microseconds for ytterbium) also provides an alternative to increase the sensitivity through time-gated spectroscopy.⁶ A common strategy to obtain NIR emission from a lanthanide ion is to form a complex with a sensitizer. The sensitizer absorbs the photons and transfers the energy to the excited states of the lanthanide for emission.⁶ The sensitizer is typically an organic compound. Over the last two decades, numerous ligands and their lanthanide complexes have been synthesized and their NIR emission properties have been examined.⁷⁻²³ However, low emission efficiency and weak absorption in the red-light region are still the bottleneck for biomedical applications.

Tetradentate porphyrin with strong absorption in the visible region is a good candidate for sensitizing lanthanide ions.²⁴ Since lanthanide ion is too big to fit inside the porphyrin ring, it usually sits above the porphyrin ring with four nitrogen atoms binding tightly to the lanthanide ion. Stability of the resulting complexes can be further enhanced by coordination of auxiliary ligands such as β -diketonate,²⁵⁻²⁹ hydroxide, chloride,³⁰ 1,10-phenanthroline,^{31, 32} 8-hydroxyquinoline,^{10, 33-35} (cyclopentadienyl)tris(dimethylphosphito)cobaltate(I),³⁶⁻³⁸ acetate,^{31, 39} and hydridotris-(pyrazol-1-yl)borate,^{40, 41} The auxiliary ligands usually do not absorb in the visible region; therefore, porphyrin is the only sensitizer. In a recent study, we found BODIPY chromophore can act as an auxiliary ligand to co-sensitize Yb³⁺ for its NIR emission.⁴² Its strong absorption at 510 nm complements the absorption of porphyrin. One of the remaining challenges is how to extend the absorption of the complex to longer wavelengths to ensure the near-infrared emission is achievable upon excitation of red-light. It should be emphasized that the red-light excitation is beneficial to medical diagnosis due to the low photobleaching effect to substrates.^{43, 44} The better penetration of red-light in biological tissues is also beneficial to *in vivo* imaging.

Recently, several lanthanide complexes of porphyrins and porpholactones with strong absorption in the red-light region have been reported. Borbas *et al*⁴⁵ studied a series of Yb³⁺ and Nd³⁺ complexes of dipicolinic acid ligand having either one or three chlorin chromophores. In comparison to previous designs,⁴⁶⁻⁴⁸ the direct linkage of chlorin to the dipicolinic acid facilitated the sensitization process. It was found that these complexes can be excited effectively in THF/water by the visible light up to 650 nm with the characteristic emission in the NIR region (980 nm for Yb³⁺ and 1064 nm for Nd³⁺) being observed. Zhang *et al*^{21, 49-56} explored various fluorinated porphyrins and porpholactones as sensitizers for the NIR emission of Yb³⁺ and a high quantum yield (63%) was obtained for a partially

^a Department of Chemistry and Biochemistry, Eastern Illinois University, Charleston, IL 61920 Email: hhe@eiu.edu. Tel: 1-217-581-6231

^b Department of Chemistry, University of South Dakota, Vermillion, SD 57069.

† Footnotes relating to the title and/or authors should appear here.

Electronic Supplementary Information (ESI) available: [details of any supplementary information available should be included here]. See DOI: 10.1039/x0xx00000x

deuterated complex in CD₂Cl₂ upon excitation at 425 nm.²¹ When the fluorinated porphodilactones were employed, the absorption of the complex extended to 636 nm (for *cis*-isomer) and 666 nm (for *trans*-isomer) enabling the potential of these complexes for NIR emission under red-light excitation.⁵⁶ Wong *et al*⁵⁷ conjugated a BODIPY functionalized ethynylphenyl group to a *meso* position or β-position of a porphyrin ring and the resulting Yb³⁺ complexes showed absorption at 624 nm. Further modification of porphyrin by a hydrophilic tetra(ethylene glycol) chain with a terminal cationic triphenylphosphonium group led to a water-soluble Yb³⁺ complex that can be used for two-photon tumor imaging.⁵⁸ In this report, we presented an alternative approach to conjugate a 4-ethynylbenzoic acid to a *meso* position of 5,15-dimesitylporphyrin and its ytterbium (III) complex as shown in Fig. 1. The absorption spectrum of the resulting complex was significantly broadened enabling sensitization of the Yb³⁺ emission with red-light.

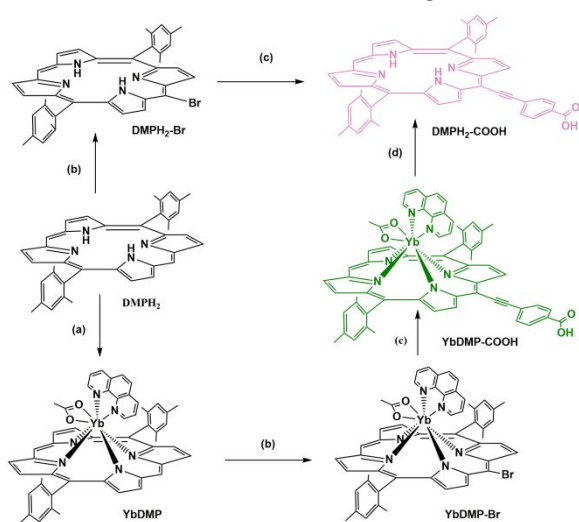


Fig. 1 Synthesis of YbDMP-COOH. Reaction conditions: (a) Yb(CH₃COO)₃·6H₂O, sulfolane, N₂, reflux, 20 minutes; 1,10-phenanthroline, 70 °C, overnight; (b) N-bromosuccinimide (NBS), dichloromethane, 0 °C, 5 hours; (c) 4-ethynylbenzoic acid, THF, [Pd(PPh₃)₄], CuI, Et₃N, 70 °C, pressure tube, 48 hr; (d) dichloromethane, TFA, r.t.

Experimental Section

Reagent and General procedures

All reagents and solvents were purchased from commercial sources and used without further purification unless otherwise stated. 2,3-Dichloro-5,6-dicyano-1,4-benzoquinone (DDQ) was supplied by Biosynth International, Inc. Tetrahydrofuran (THF), dimethylformamide (DMF), deuterated chloroform (CDCl₃), N-bromosuccinimide (NBS), copper(I) iodide (CuI), tetrakis(triphenylphosphine)palladium (0) (Pd(PPh₃)₄), 2,4-dimethylpyrrole and mesitaldehyde were purchased from ACROS Organics and used directly without further purification. 2,2'-dipyrrromethane was synthesized based upon a method developed in our lab and its structure was confirmed by ¹H NMR. The 230-400 mesh silica gel was purchased from Dynamic Adsorbents, Inc. ¹H NMR spectra were recorded on a 400 MHz Bruker Avance II-NMR spectrometer, using ACROS Organics

chloroform-d 99.8% D, containing 0.03% (v/v) TMS as the internal reference. All ¹H NMR signals were referenced to TMS. The chemical shifts were reported in parts per million (ppm). For the signal splitting, the following abbreviations are used: *s*, singlet; *d*, doublet; *t*, triplet; *m*, multiplet; *bs*, broad singlet. UV-Vis absorption spectra were performed on a Cary 100 Series UV-Vis Dual Beam spectrophotometer over a range of 200 - 800 nm. 5,15-Dimesitylporphyrin (DMPH₂) and 5-bromo-10,20-dimesitylporphyrin (Br-DMP) were synthesized according to a literature method⁵⁹ and its structure was confirmed by ¹H NMR.

Synthesis of DMPH₂-COOH

To a 50 mL Shlenk flask was added Br-DMPH₂ (0.10 g, 0.16 mmol) 4-ethynylbenzoic acid (0.046 g, 0.32 mmol), Pd(PPh₃)₄ (10 mg, 0.0086 mmol, 5%), CuI (1.6 mg, 0.0086 mmol, 5%) and Et₃N (2 mL) in THF (20 mL) in a pressure tube inside the glovebox. The pressure tube was sealed and heated at 80°C for two days. Major band was collected after flushing with CHCl₃:MeOH 200:1. Yield: 85 mg, 77%. ¹H NMR (400MHz, DMSO-d₆) δ 13.23(s, 1H, ^kH), 10.47(s, 1H, ^aH), 9.85 (d, 2H, ^bH), 9.51 (d, 2H, ^cH), 8.75 (d, 2H, ^eH), 8.67 (d, 2H, ^dH), 7.40 (s, ^hH), 2.67 (s, 6H, ⁱH), 1.79 (s, 12H, ^jH), -2.60 (s, 2H, ^lH). ESI-HR-MS: 691.3058 (M+H) (Calcd. 691.3073).

Synthesis of YbDMP.

To a 50 mL Shlenk flask was added DMPH₂ (0.22 g, 0.40 mmol), Yb(CH₃COO)₃·4H₂O (0.21 g, 0.49 mmol) in sulfolane (20 mL). The flask was put on a heating block and the mixture was refluxed for 45 minutes under nitrogen. Then 1,10-phenanthroline (0.160 g, 0.82 mmol) was added when the temperature decreased to about 70°C. The solution was magnetically stirred at 70 °C overnight. Then, 30 mL dichloromethane (DCM) was added to the flask when the temperature of the mixture decreased to room temperature. The solution was washed twice by water. Organic layer was collected. The solution was concentrated to about 10 mL on a rotor evaporator and then was loaded to the column for purification. The column was first eluted with DCM to remove all unreacted DMPH₂, and then with DCM/MeOH: 100:5 (V/V). The major band was collected as the product. After recrystallization from DCM/MeOH, 0.14 g YbDMP was obtained. C₅₂H₄₃N₆O₂Yb: Calcd. C 66.05, H 4.51, N 9.06. Found: C 66.35, H 4.63, N 9.28. ESR-MS: 898.2697 (M-CH₃COO) (Calcd. 898.2703).

Synthesis of YbDMP-COOH

To a 50 mL Shlenk flask was added Br-DMPH₂ (0.11 g, 0.17 mmol), Yb(CH₃COO)₃·4H₂O (0.10 g, 0.26 mmol) in sulfolane (20 mL). The flask was put on a heating block refluxing under nitrogen for 45 minutes. Then added 30 mL dichloromethane to the flask when the temperature decreased to room temperature and the solution washed by water thoroughly twice. After removing all DCM, the solid was collected. After drying, the sample was loaded to the column for purification. The column was first eluted with DCM to remove all unreacted DMPH₂-Br, then with DCM/MeOH: 100:10. The major band was collected. After removed all solvent, the solid (0.18 g) was dissolved in 50 mL toluene, and 1,10-phenanthroline (0.040 g,

0.22 mmol) was added and the mixture was stirred overnight at room temperature. Then the solvent was removed and added methanol to get the solid product (49.7 mg, 0.0483 mmol). The solid was dried and transferred to a 50 mL pressure tube and ethynylbenzoic acid (7 mg, 0.047 mmol), Pd(PPh₃)₄ (3 mg, 0.0024 mmol, 5%), CuI (1.0 mg, 0.0086 mmol, 5%), Et₃N (4 mL) and dry THF (20 mL) were added inside a glovebox. The tube was sealed and refluxed at 80°C for two days. After the tube was cooled to the room temperature, all solvent was removed, and the sample was loaded on the column for purification using DCM/MeOH (100:2). The major band was collected as the product. Yield: 14 mg. C₆₁H₄₇N₆O₄Yb: Calcd. C 66.54, H 4.30, N 7.63. Found: C 66.40, H 4.51, N 7.56. MS (MALDI): 1042.246 (M-CH₃COO) (Calcd. 1042.291).

X-ray crystallographic analysis

Single crystals were obtained from slow evaporation of a dichloromethane/methanol solution at room temperature. The crystals were mounted on glass fiber for data collection. Diffraction measurements were made on a CCD-based commercial X-ray diffractometer using Mo K α radiation ($\lambda = 0.71073 \text{ \AA}$). The frames were collected at 100K with a scan width 0.3° in ω and integrated with the Bruker SAINT software package⁶⁰ using the narrow-frame integration algorithm. The unit cell was determined and refined by least-squares upon the refinement of XYZ-centeroids of reflections above 20 θ (I). The data were corrected for absorption using SADABS program.⁶¹ The structures were refined on F^2 using the SHELXL97.⁶² Crystal data for YbDMP·0.65 CH₂Cl₂·1.82 CH₃OH: C_{54.47} H_{50.76} Cl_{1.30} N₆ O_{3.82} Yb, MW = 1069.66, monoclinic, space group = $P_{21/c}$, $a = 11.3239(9)$, $b = 16.5128(14)$, $c = 25.834(2) \text{ \AA}$, $\beta = 93.6710(10)^\circ$, $V = 4820.7(7) \text{ \AA}^3$, $Z = 4$, $\rho_{\text{calcd.}} = 1.474 \text{ Mgm}^{-3}$, $\mu = 2.064 \text{ mm}^{-1}$, $F(000) = 2169$, $T = 100(2) \text{ K}$. 47802 reflections were measured, of which 8942 were unique ($R_{\text{int}} = 0.0477$). Final $R_1 = 0.0608$ and $wR_2 = 0.1187$ were obtained for 7583 observed reflections with $I > 2\sigma(I)$, 609 parameters, and GOF = 1.156. CCDC#: 1944838

Photophysical measurements

Absorption spectra were obtained on a Cary100 UV-visible spectrophotometer at room temperature using a 1-cm quartz cuvette. Steady-state and time-resolved spectroscopy studies were performed on an F55 fluorimeter (Edinburg Instruments) with a Xenon arc lamp as a light source. For the visible emission measurements, the slit width for emission and excitation arms was 1 nm. For the NIR emission, the slit width for both emission and excitation was 8 nm. The fluorescence quantum yield, ϕ_x , in the visible region was measured using the following equation:

$$\phi_x = \phi_{\text{ST}} \left[\frac{\text{Grad}_x}{\text{Grad}_{\text{ST}}} \right] \left[\frac{n_x}{n_{\text{ST}}} \right]^2$$

where Grad the gradient from the plot of integrated fluorescence intensity vs absorbance of five samples with different concentrations, and n is the refractive index of the solvents. Rhodamine 6G in ethanol ($\phi_{\text{ST}} = 0.95$, $\lambda_{\text{ex}} = 480 \text{ nm}$)⁶³ was used as a reference for visible emission and YbTPPTp^H was used as a reference for NIR emission ($\phi_{\text{ST}} = 0.032$, $\lambda_{\text{ex}} = 540 \text{ nm}$).⁴⁰ The decay curves of the samples were also measured on the F55 (Edinburg Instruments) spectrometer. A laser diode EPL

375 (Edinburg Instruments) with a wavelength of 375 nm was used as a light source. The NIR decay curves were acquired using an optical parametric oscillator (OPOTEK Opolette) as an excitation source. NIR emission was detected using a 0.3 m flat-field monochromator (Jobin Yvon TRIAX 320) equipped with a NIR-sensitive photomultiplier tube (Hamamatsu R2658P) in a cooled housing (Products for Research). All spectra were corrected for instrument response. The output from the photomultiplier was pre-amplified (Stanford Research SR 445A) and fed to a multichannel scaler (Stanford Research SR 430) for time-resolved photon counting. The entire system was PC controlled using LabView software.

Theoretical calculation

All calculations were performed at a density functional theory (DFT) level using Gaussian 09 software.⁶⁴ The initial input structures were built based upon the crystal structure of a similar complex. The ground state geometries of compounds were optimized using 6-31G(d) as a basis set for C, H, N, and MWB28 for Yb. All other parameters were default set. No negative frequency was found in the final optimized structures. All calculations were carried out in the SMD model for mimicking the solvent effect. The time-dependent (TD) DFT calculations were carried out using the same basis sets and functional in dichloromethane. The calculated absorption data were analyzed by GaussSum software.⁶⁵

Results and Discussion

Synthesis and Characterization

The YbDMP-COOH was prepared from a three-step synthetic route as shown in Fig. 1. DMPH₂ was synthesized according to the literature method⁶⁶ and characterized by ¹H NMR. It was then refluxed with Yb(CH₃COO)₃·4H₂O in sulfolane under a nitrogen atmosphere. The completion of the reaction was monitored by thin-layer chromatography. After the reaction, two molar equivalents of 1,10-phenanthroline were added to the solution at 70 °C and the solution was magnetically stirred overnight. After adding dichloromethane, the solution was washed successively with water to remove sulfolane and the solid was subjected to column chromatography for purification. The pure YbDMP was obtained as a purple powder after crystallization from methanol. This compound was then subjected to the N-bromosuccinimide (NBS) in chloroform to afford the YbDMP-Br. In the final step, YbDMP-Br was reacted with 1.2 molar equivalents of ethynylbenzoic acid under conventional Sonogashira cross-coupling condition in a pressure tube for two days to result in the target product YbDMP-COOH as a dark green powder. The free ligand DMPH₂-COOH was prepared by either direct bromination of DMPH₂ and subsequent Sonogashira cross-coupling with ethynylbenzoic acid (route 1) or hydrolyzation of YbDMP-COOH in trifluoroacetic acid/dichloromethane solution (route 2). We found the route 1 is more convenient and cost-effective. It should be noted that the direct reaction between DMPH₂-COOH with Yb³⁺ was unsuccessful due to the instability of DMPH₂-COOH at high

temperature; the ligand was decomposed. The complex YbDMP-COOH is quite stable in air and is soluble in DMSO, DMF, dichloromethane, chloroform, toluene, slightly soluble in ethanol and methanol, and insoluble in hexane and water. Its composition was confirmed by elemental analysis and mass spectroscopy. The characteristic vibrational peaks at 1604 cm^{-1} for $\nu(\text{C}=\text{O})$, 3424 cm^{-1} for $\nu(\text{COOH})$ and 2186 cm^{-1} $\nu(\text{C}\equiv\text{C})$ were observed in the YbDMP-COOH. We were unable to obtain the high-quality crystals for this complex; however, the structure of YbDMP was ascertained by single-crystal X-ray diffraction analysis as shown in Fig. 2. The Yb^{3+} is above the porphyrin ring and coordinated by four N atoms from the porphyrin ring, two N from 1,10-phenanthroline, and two O atoms from acetate ion. The coordination geometry is quite similar to its analogs that we reported early.³⁹ We envision that the major structural characteristics of YbDMP will remain in the YbDMP-COOH as shown in Fig. 3 from the theoretical calculation. The bond length and bond angles are quite close to the crystal structure of YbDMP. Phenylacetylene moiety was slightly tilted against the porphyrin ring. It should be noted that the preparation of GdDMP-COOH and LuDMP-COOH was unsuccessful. GdDMP and LuDMP both decomposed during their coupling with 4-ethynylbenzoic acid under Sonogashira coupling reaction conditions.

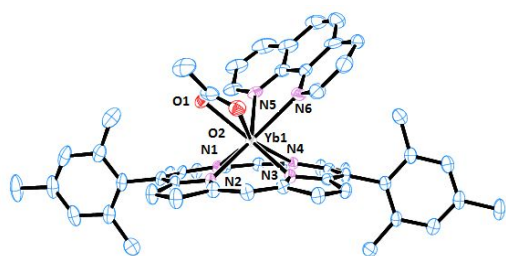


Fig. 2 ORTEP diagram of YbDMP with 50% thermal ellipsoid probability. Hydrogen atoms were omitted for clarity.

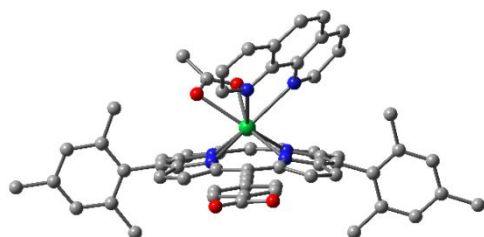


Fig. 3 Geometry-optimized structure of YbDMP-COOH. Color code: grey: C; blue: N; red: O. Hydrogen atoms were omitted for clarity.

Photophysical Properties

The absorption of YbDMP-COOH extends to the red region. The absorption spectrum of YbDMP-COOH in dichloromethane is shown in Fig. 4 with key photophysical data in Table 1. Data for DMPH₂-COOH and YbDMP were also included for comparison. The free base DMPH₂-COOH exhibits broader absorption compared to its ytterbium complex due to its lower symmetry according to Gouterman's theory.⁶⁷ Four peaks in the Q band region were observed with 660 nm on the far right side. The Soret band for YbDMP-COOH was centered at 439 nm, which is red-shifted 26 nm compared to YbDMP. The absorbance at the

Soret was much lower than that of YbDMP. In the Q band region, the overall absorption was enhanced with two peaks centered at 568 nm and 615 nm, both are also red-shifted compared to a single peak at 544 nm for YbDMP. The red-shift of the absorption derives from the formation of a larger π -conjugation system after the 4-ethynylbenzoic acid was linked to the porphyrin ring. Such a shift has been observed in its zinc analogs. The DMPH₂-COOH showed strong emission ($\Phi = 3.9\%$) in the visible region with two peaks at 662 and 732 nm, whereas its Yb^{3+} complex gave very weak emission ($\Phi = 0.23\%$) with three peaks at 619, 662, and 732 nm (Table S2). TD-DFT calculations for the DMPH₂-COOH showed the emission was mainly from HOMO→LUMO transition.

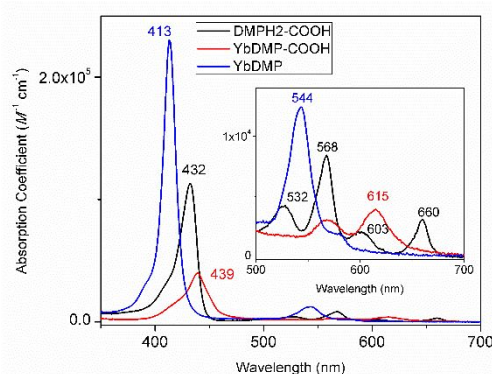


Fig. 4 Absorbance spectra of DMPH₂-COOH, YbDMP and YbDMP-COOH in DCM at room temperature. The concentration was 3.50×10^{-6} mol/L.

Table 1. Photophysical properties of YbDMP and YbDMP-COOH in CH₂Cl₂ at room temperature.

	YbDMP	YbDMP-COOH	DMPH ₂ -COOH
<i>VIS Region</i>			
Abs. (ϵ)	413 (2.3×10^5) 544 (1.2×10^4)	439 (4.0×10^4) 568 (3.1×10^3) 615 (4.0×10^3)	432 (1.1×10^5) 528 (4.2×10^3) 568 (8.4×10^3) 603 (2.1×10^3) 660 (3.1×10^3)
Emission (nm)	648, 699	662, 732	619, 662, 732
τ (ns) ^a , QY (%) ^b	7.92, 0.89	5.63, 0.23	7.60, 3.9
<i>NIR Region</i>			
Emission (nm)	975, 1003	978, 1006	-
τ (μ s) ^c , QY (%) ^d	10.5, 2.2 \pm 0.1	12.0, 2.3 \pm 0.1	-

^a $\lambda_{\text{ex}} = 375\text{ nm}$; ^bThe TPPH₂ was used as a reference (QY = 0.11 in benzene); ^c $\lambda_{\text{ex}} = 510\text{ nm}$. ^dThe YbTPPT_p^H was used as a reference (QY = 0.032 in dichloromethane).⁴⁰

YbDMP-COOH exhibits characteristic Yb^{3+} emission in the NIR region upon excitation. As shown in Fig. 5(A), the spectrum shows two characteristic peaks centered at 978 and 1006 nm, which correspond to the transition of ${}^2F_{5/2} \rightarrow {}^2F_{7/2}$. The appearance of multiple peaks could be due to the M_J splitting of the ground state and or emitting states.⁶ The emission intensities at 978 and 1006 nm are very close to each other, indicating an eight-coordinating environment around Yb^{3+} ion as we observed previously.³⁹ The very close emission intensities were also observed in YbDMP. The overall emission intensities

are dependent upon the excitation wavelength. As shown in **Fig. 5(B)**, the emission intensity is almost doubled with a $\lambda_{\text{ex}} = 448$ nm compared to intensities with $\lambda_{\text{ex}} = 541, 568,$ and 616 nm. However, in the longer wavelength, the excitation at 568 and 610 nm produced higher emission intensity than 541 nm since YbDMP-COOH has much weaker absorption at 541 nm. YbDMP can also be excited under the visible light excitation, however, the emission intensity is very low when the excitation moves to a longer wavelength ($\lambda_{\text{ex}} > 550$ nm).

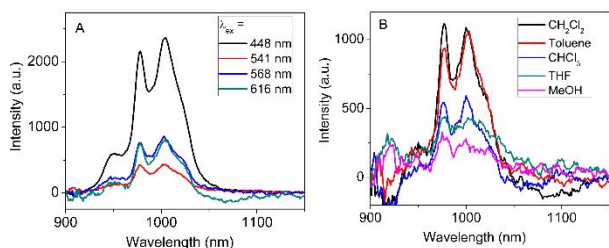


Fig. 5 (A) NIR emission of YbDMP-COOH under different excitation wavelengths in dichloromethane and (B) in different solvents ($\lambda_{\text{ex}} = 616$ nm) at room temperature. The concentration was 3.24×10^{-5} mol/L.

The NIR emission is the result of “antenna” effect. In general, the energy from the porphyrin transfers to the excited state of the Yb^{3+} for its NIR emission. **Fig. 6(A)** shows the emission spectra of DMPH₂-COOH (free porphyrin), YbDMP and YbDMP-COOH in DCM under the same concentration. The fluorescence intensity of YbDMP-COOH in the visible region was less than 2% of DMPH₂-COOH, indicating a dramatic fluorescence quenching of DMPH₂-COOH after the formation of the complex. Such a decrease is most likely from an energy transfer from the porphyrin to the excited state of $\text{Yb}(\text{III})$. **Fig. 6(B)** shows the absorption and the excitation spectra of YbDMP-COOH in DCM. The absorption spectrum was similar to the Yb^{3+} excitation spectrum, indicating again that the porphyrin sensitized Yb^{3+} emission. The measured quantum yield in the NIR region (2.30%) is quite similar to $\text{YbTPPT}_p^{\text{H}}$ ⁴⁰ and is slightly higher than YbDMP (2.21%). To probe the energy transfer time scale, the complex was adsorbed on TiO_2 nanoparticles and SiO_2 nanoparticles through benzoic acid.^{68, 69} It was found that the complex showed very weak emission on TiO_2 compared to SiO_2 as shown in **Fig. 6A** due to efficient fluorescence quenching of the electron transfer from the porphyrin ring to the TiO_2 conduction band, which did not occur for SiO_2 . This indicates the energy transfer from porphyrin to the Yb^{3+} is comparable to the TiO_2 nanoparticle, which is typically 500 fs.⁷⁰⁻⁷²

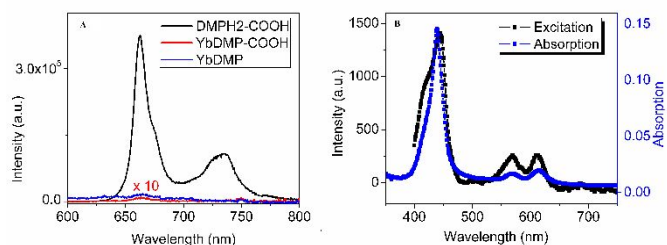


Fig. 6 (A) Emission spectrum of DMPH₂-COOH, YbDMP-COOH and YbDMP in dichloromethane ($\lambda_{\text{ex}} = 375$ nm), (B) Absorption and excitation of YbDMP-COOH in dichloromethane ($\lambda_{\text{em}} = 1004$ nm). The concentration was 3.65×10^{-5} mol/L for absorption and excitation, respectively.

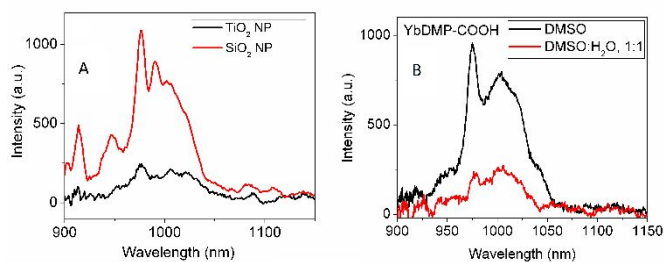


Fig. 7 (A) NIR emission spectra of YbDMP-COOH on TiO_2 and SiO_2 nanoparticles ($\lambda_{\text{ex}} = 445$ nm); (B) NIR emission spectra of YbDMP-COOH and YbDMP upon excitation at 633 nm in DMSO/water (1:1).

Lastly, the emission upon excitation at 633 nm aqueous solution (DMSO:H₂O, 1:1) was examined. This wavelength is chosen due to its commercial availability either as HeNe laser (632.8 nm) or diode laser (633 nm). As shown in **Fig. 7B**, upon excitation at 633 nm, characteristic emission at 978 nm was observed, which is indicative of potential medical diagnostic applications. However, the emission intensity decreased about 70% compared to the emission in pure DMSO. This decrease could be ascribed to interaction of solvent with metal ion. It was found that the NIR emission of YbDMP-COOH in CH_3OH and THF was also quite weak than that in toluene, DCM and DMF indicating the interaction of solvent with Yb^{3+} center in the complex. The lifetime at 978 nm in CH_3OH and CD_3OD were 1.50 μs and 7.29 μs , respectively. Using the equation $q_{\text{Yb}} = 2(\kappa_{\text{CH}_3\text{OH}} - \kappa_{\text{CD}_3\text{OD}} - B)$,⁷³ the estimated $q_{\text{Yb}} \approx 1$, if B is between 0.05 and 0.1. This indicated that one solvent molecule may have very close contact with the Yb center. This is reasonable due to the fact that the Yb center is pretty open compared to tetraphenylporphyrin analogues, in which 5, 10, 15 and 20 positions were all occupied by almost vertically aligned phenyl groups. This is not the case for YbDMP-COOH, in which two meso positions have phenyl substituents, third one has a flat ethynylbenzoic acid group and the last one has no substituent leaving an open space for solvent molecules to access. This provided opportunities for solvent molecules to access to inner-coordination sphere; and therefore, quench the NIR emission. The low water solubility of the sample prevented further evaluation of the NIR emission capability in water. In an attempt to prepare an aqueous solution by dissolving the DMSO solution into water for further assessment, the resulting mixture was becoming cloudy when the water/DMSO ratio (V/V) increased to 2:1, and the sample quickly precipitated from the mixture, making the measurement unreliable. No NIR emission was observed from the mixture. It is worth noting that it is important to evaluate the sample in the cell, unfortunately, the poor solubility and lack of the facility in our lab prevented us from further study. We are currently developing new strategies to address this challenge.

Conclusions

In summary, a green Yb^{3+} porphyrin with strong absorption at 615 nm was synthesized by appending a 4-ethynylbenzoic acid to a *meso* position of a porphyrin. The complex showed

characteristic emission in the NIR region upon excitation at 633 nm in DMSO/water, demonstrating its potential in medical diagnostic applications.

Conflicts of interest

There are no conflicts to declare

Acknowledgements

HH thanks National Science Foundation (Award # 1507871) and The Extreme Science and Engineering Discovery Environment (XSEDE) (CHE130116) for financial support of this work.

Notes and references

§These authors contribute equally

† Electronic Supplementary Information (ESI) available: syntheses of DMPH₂-Br, ¹H NMR and ESI-MS of DMPH₂-COOH, ESIMS of YbDMP, MALDI MS of YbDMP-COOH, decay profiles for YbDMP-COOH, YbDMP in DCM, YbDMP-COOH in CD₃OD and in CH₃OH, molecular orbital profiles of HOMO and LUMO for YbDMP-COOH, DMPH₂-COOH and YbDMP, FT-IR spectra of YbDMP, DMPH₂-COOH and YbDMP-COOH, and normalized emission spectra of DMPH₂-COOH and YbDMP-COOH, and emission spectra of DMPH₂-COOH, and TPPH₂ in DCM. See DOI: 10.1039/b000000x/

‡ Footnotes should appear here. These might include comments relevant to but not central to the matter under discussion, limited experimental and spectral data, and crystallographic data.

1. K. P. Carter, A. M. Young and A. E. Palmer, *Chem. Rev.*, 2014, **114**, 4564-4601.
2. J. Zhou, Q. Liu, W. Feng, Y. Sun and F. Li, *Chem. Rev.*, 2014.
3. A. T. Bui, M. Beyler, A. Grichine, A. Duperray, J. C. Mulatier, Y. Guyot, C. Andraud, R. Tripier, S. Brasselet and O. Maury, *Chem Commun (Camb)*, 2017, **53**, 6005-6008.
4. J.-C. G. Bünzli, *Chem. Rev.*, 2010, **110**, 2729-2755.
5. G. K. Liu and X. Y. Chen, in *Handbook on the Physics and Chemistry of Rare Earths*, ed. J. C. G. B. K. A. Gschneidner Jr., and V. K. Pecharsky, North-Holland, Amsterdam, 2007, vol. 37, pp. 99-170.
6. S. Comby and J.-C. G. Bünzli, in *Handbook on the Physics and Chemistry of Rare Earths*, eds. J. Karl A. Gschneidner, J.-C. G. Bünzli and V. K. Pecharsky, Elsevier, 2007, vol. 37, pp. 217-470.
7. E. G. Moore, G. Szigethy, J. Xu, L.-O. Pålsson, A. Beeby and K. N. Raymond, *Angew. Chem. Int. Ed.*, 2008, **47**, 9500-9503.
8. M. Feng, F. Pointillart, B. LeGuennic, B. Lefeuvre, S. Golhen, O. Cador, O. Maury and L. Ouahab, *Chem. Asian J.*, 2014, **9**, 2814 – 2825.
9. F. Artizzu, F. Quochi, L. Marchiò, E. Sessini, M. Saba, A. Serpe, A. Mura, M. L. Mercuri, G. Bongiovanni and P. Deplano, *J. Phys. Chem. Lett.*, 2013, **4**, 3062-3066.
10. S. Comby, S. A. Tuck, L. K. Truman, O. Kotova and T. Gunnlaugsson, *Inorg. Chem*, 2012, **51**, 10158-10168.
11. N. Iki, S. Hiro-oka, T. Tanaka, C. Kabuto and H. Hoshino, *Inorg. Chem*, 2012, **51**, 1648-1656.
12. J. H. Ryu, Y. K. Eom, J.-C. G. Bünzli and H. K. Kim, *New J. Chem.*, 2012, **36**, 723-731.
13. F. Caillé, C. S. Bonnet, F. Buron, S. Villette, L. Helm, S. Petoud, F. Suzenet and É. Tóth, *Inorg. Chem.*, 2012, **51**, 2522-2532.
14. A. M. Nonat, C. m. Allain, S. Faulkner and T. Gunnlaugsson, *Inorg. Chem.*, 2010, **49**, 8449-8456.
15. F.-F. Chen, Z.-Q. Bian, B. Lou, E. Ma, Z.-W. Liu, D.-B. Nie, Z.-Q. Chen, J. Bian, Z.-N. Chen and C.-H. Huang, *Dalton Trans.*, 2008, 5577-5583.
16. X.-L. Li, F.-R. Dai, L.-Y. Zhang, Y.-M. Zhu, Q. Peng and Z.-N. Chen, *Organometallics*, 2007, **26**, 4483-4490.
17. N. M. Shavaleev, R. Scopelliti, F. Gumy and J.-C. G. Bünzli, *Inorg. Chem*, 2009, **48**, 7937-7946.
18. K. Norton, G. A. Kumar, J. L. Dilks, T. J. Emge, R. E. Riman, M. G. Brik and J. G. Brennan, *Inorg. Chem*, 2009, **48**, 3573-3580.
19. W. Huang, D. Wu, D. Guo, X. Zhu, C. He, Q. Meng and C. Duan, *Dalton Trans.*, 2009, 2081-2084.
20. A. de Bettencourt-Dias, P. S. Barber and S. Bauer, *J. Am. Chem. Soc.*, 2012, **134**, 6987-6994.
21. J.-Y. Hu, Y. Ning, Y.-S. Meng, J. Zhang, Z.-Y. Wu, S. Gao and J.-L. Zhang, *Chem. Sci.*, 2017, **8**, 2702-2709.
22. C. Y. Chow, S. V. Eliseeva, E. R. Trivedi, T. N. Nguyen, J. W. Kampf, S. Petoud and V. L. Pecoraro, *J Am Chem Soc*, 2016, **138**, 5100-5109.
23. E. R. Trivedi, S. V. Eliseeva, J. Jankolovits, M. M. Olmstead, S. Petoud and V. L. Pecoraro, *J. Am. Chem. Soc.*, 2014, **136**, 1526-1534.
24. H. He, *Coord. Chem. Rev.*, 2014, **273-274**, 87-99.
25. Z. Ahmed and K. Iftikhar, *Dalton Trans.*, 2019, **48**, 4973-4986.
26. H. P. Santos, E. S. Gomes, M. V. dos Santos, K. A. D'Oliveira, A. Cuin, J. S. Martins, W. G. Quirino and L. F. Marques, *Inorg. Chem. Acta*, 2019, **484**, 60-68.
27. S. Fan, X. Yao, J. Li, W. Li and G. Li, *J. Lumin.*, 2018, **203**, 473-480.
28. A. Swinburne, M. Langford Paden, T. Chan, S. Randall, F. Ortu, A. Kenwright and L. Natrajan, *Inorganics*, 2016, **4**, 27.
29. T. M. George, S. Varughese and M. L. P. Reddy, *RSC Advances*, 2016, **6**, 69509-69520.
30. H. He, X. Zhu, A. Hou, J. Guo, W.-K. Wong, W.-Y. Wong, K.-F. Li and K.-W. Cheah, *Dalton Trans.*, 2004, **23**, 4064-4073.
31. H. He, M. Dubey, A. G. Sykes and P. S. May, *Dalton Trans.*, 2010, 6466-6474.
32. H. He, P. S. May and D. Galipeau, *Dalton Trans.*, 2009, 4766-4771.
33. H. He, A. Gurung and L. Si, *Chem. Comm.*, 2012, **48**, 5910-5912.
34. D. Imbert, S. Comby, A.-S. Chauvin and J.-C. G. Bünzli, *Chem. Comm.*, 2005, 1432-1434.
35. H. He, L. Si, Y. Zhong and M. Dubey, *Chem. Commun.*, 2012, **48**, 1886-1888.
36. W.-K. Wong, X. Zhu and W.-Y. Wong, *Coord. Chem. Rev.*, 2007, **251**, 2386-2399
37. S. Zhao, X. Liu, W.-Y. Wong, X. Lü and W.-K. Wong, *Inorg. Chem. Acta*, 2014, **414**, 160-164.
38. T. Zhang, X. Zhu, C. C. W. Cheng, W.-M. Kwok, H.-L. Tam, J. Hao, D. W. J. Kwong, W.-K. Wong and K.-L. Wong, *J. Am. Chem. Soc.*, 2011, **133**, 20120-20122.

39. H. He, A. G. Sykes, P. S. May and G. He, *Dalton Trans.*, 2009, 7454-7461.
40. T. J. Foley, B. S. Harrison, A. S. Knefely, K. A. Abboud, J. R. Reynolds, K. S. Schanze and J. M. Boncella, *Inorg. Chem.*, 2003, **42**, 5023-5032.
41. H. He, J. Guo, Z. Zhao, W.-K. Wong, W.-Y. Wong, W.-K. Lo, K.-F. Li, L. Luo and K.-W. Cheah, *Eur. J. Inorg. Chem.*, 2004, 837-845.
42. H. He, J. D. Bosonetta, K. A. Wheeler and S. P. May, *Chem. Comm.*, 2017, 10120-10123.
43. Z. Zhang, Y. Zhou, H. Li, T. Gao and P. Yan, *Dalton Trans.*, 2019, **48**, 4026-4034.
44. J. Xu, A. Gulzar, P. Yang, H. Bi, D. Yang, S. Gai, F. He, J. Lin, B. Xing and D. Jin, *Coord. Chem. Rev.*, 2019, **381**, 104-134.
45. R. Xiong, D. Mara, J. Liu, R. Van Deun and K. E. Borbas, *J. Am. Chem. Soc.*, 2018, **140**, 10975-10979.
46. W. Qianming, S. Shin-ichi and T. Hitoshi, *Chem. Lett.*, 2009, **38**, 648-649.
47. J. Laakso, G. A. Rosser, C. Szijjártó, A. Beeby and K. E. Borbas, *Inorg. Chem.*, 2012, **51**, 10366-10374.
48. R. Xiong, J. Andres, K. Scheffler and K. E. Borbas, *Dalton Trans.*, 2015, **44**, 2541-2553.
49. Y. Ning, Y.-W. Liu, Y.-S. Meng and J.-L. Zhang, *Inorg. Chem.*, 2018, **57**, 1332-1341.
50. Y. Ning, Y. W. Liu, Z. S. Yang, Y. Yao, L. Kang, J. L. Sessler and J. L. Zhang, *J. Am. Chem. Soc.*, 2020, **142**, 6761-6768.
51. G.-Q. Jin, Y. Ning, J.-X. Geng, Z.-F. Jiang, Y. Wang and J.-L. Zhang, *Inorg. Chem. Frontiers*, 2020, **7**, 289-299.
52. Y. Ning, S. Cheng, J.-X. Wang, Y.-W. Liu, W. Feng, F. Li and J.-L. Zhang, *Chem. Sci.*, 2019, **10**, 4227-4235.
53. Y. Ning, G.-Q. Jin and J.-L. Zhang, *Acc. Chem. Res.*, 2019, **52**, 2620-2633.
54. Y. Ning, M. Zhu and J.-L. Zhang, *Coord. Chem. Rev.*, 2019, **399**, 213028.
55. Y. Ning, J. Tang, Y.-W. Liu, J. Jing, Y. Sun and J.-L. Zhang, *Chem. Sci.*, 2018, **9**, 3742-3753.
56. Y. Ning, X.-S. Ke, J.-Y. Hu, Y.-W. Liu, F. Ma, H.-L. Sun and J.-L. Zhang, *Inorg. Chem.*, 2017, **56**, 1897-1905.
57. T. Zhang, X. Zhu, W.-K. Wong, H.-L. Tam and W.-Y. Wong, *Chem. Eur. J.*, 2013, **19**, 739-748.
58. T. Zhang, R. Lan, L. Gong, B. Wu, Y. Wang, D. W. J. Kwong, W.-K. Wong, K.-L. Wong and D. Xing, *ChemBioChem*, 2015, **16**, 2357-2364.
59. L. Si, H. He and K. Zhu, *New J. Chem.*, 2014, **38**, 1565-1572.
60. SAINT+ ver 6.02a, Bruker Analytical X-ray System, Inc., Madison, WI, 1998.
61. G. M. Sheldrick, in *SADABS, Empirical Absorption Correction Program; University of Göttingen, Germany*, 1997.
62. G. M. Sheldrick, in *SHELXTLTM, Reference manual, Version 5.1 Madison, WI*, 1997.
63. R. F. Kubin and A. N. Fletcher, *J. Lumin.*, 1982, **27**, 455-462.
64. M. J. T. Frisch, G. W.; Schlegel, H. B.; Scuseria, G. E.; Robb, M. A.; Cheeseman, J. R.; Scalmani, G.; Barone, V.; Mennucci, B.; Petersson, G. A.; Nakatsuji, H.; Caricato, M.; Li, X.; Hratchian, H. P.; Izmaylov, A. F.; Bloino, J.; Zheng, G.; Sonnenberg, J. L.; Hada, M.; Ehara, M.; Toyota, K.; Fukuda, R.; Hasegawa, J.; Ishida, M.; Nakajima, T.; Honda, Y.; Kitao, O.; Nakai, H.; Vreven, T.; Montgomery, Jr., J. A.; Peralta, J. E.; Ogliaro, F.; Bearpark, M.; Heyd, J. J.; Brothers, E.; Kudin, K. N.; Staroverov, V. N.; Kobayashi, R.; Normand, J.; Raghavachari, K.; Rendell, A.; Burant, J. C.; Iyengar, S. S.; Tomasi, J.; Cossi, M.; Rega, N.; Millam, N. J.; Klene, M.; Knox, J. E.; Cross, J. B.; Bakken, V.; Adamo, C.; Jaramillo, J.; Gomperts, R.; Stratmann, R. E.; Yazyev, O.; Austin, A. J.; Cammi, R.; Pomelli, C.; Ochterski, J. W.; Martin, R. L.; Morokuma, K.; Zakrzewski, V. G.; Voth, G. A.; Salvador, P.; Dannenberg, J. J.; Dapprich, S.; Daniels, A. D.; Farkas, Ö.; Foresman, J. B.; Ortiz, J. V.; Cioslowski, J.; Fox, D. J., Gaussian, Inc., Wallingford CT, 2009.
65. N. M. O'Boyle, A. L. Tenderholt and K. M. Langner, *J. Comp. Chem.*, 2008, **29**, 839-845.
66. M. Yanagida, L. P. Singh, K. Sayama, K. Hara, R. Katoh, A. Islam, H. Sugihara, H. Arakawa, M. K. Nazeeruddin and M. Grätzel, *Dalton Trans.*, 2000, 2817-2822.
67. M. Gouterman, in *The Porphyrins*, ed. D. Dolphin, Academic Press, New York, 1978, vol. 3, pp. 1-65.
68. L. L. Li and E. W. Diau, *Chem. Soc. Rev.*, 2013, **42**, 291-304.
69. L. Luo, C.-F. Lo, C.-Y. Lin, I. J. Chang and E. W.-G. Diau, *The Journal of Physical Chemistry B*, 2005, **110**, 410-419.
70. C.-W. Chang, L. Luo, C.-K. Chou, C.-F. Lo, C.-Y. Lin, C.-S. Hung, Y.-P. Lee and E. W.-G. Diau, *J. Phy. Chem. C.*, 2009, **113**, 11524-11531.
71. T. Higashino and H. Imahori, *Dalton Trans.*, 2015, **44**, 448-463.
72. A. Hagfeldt, G. Boschloo, L. Sun, L. Kloo and H. Pettersson, *Chem Rev*, 2010, **110**, 6595-6663.
73. A. Beeby, I. M. Clarkson, R. S. Dickins, S. Faulkner, D. Parker, L. Royle, A. S. de Sousa, J. A. M. Williams and M. Woods, *J. Chem. Soc. Perkin Trans. 2*, 1999, 493-504.